nature neuroscience

SUPPLEMENTARY INFORMATION

https://doi.org/10.1038/s41593-017-0038-4

In the format provided by the authors and unedited.

Stress-induced unfolded protein response contributes to Zika virus–associated microcephaly

Ivan Gladwyn-Ng[1], Lluís Cordón-Barris[1], Christian Alfano[1], Catherine Creppe[1], Thérèse Couderc[2,3], Giovanni Morelli[1,4], Nicolas Thelen[1], Michelle America[1], Bettina Bessières[5,6], Férechté Encha-Razavi[5], Maryse Bonnière[5], Ikuo K. Suzuki[7], Marie Flamand[8], Pierre Vanderhaeghen[7,9], Marc Thiry[1], Marc Lecuit[2,3,10]* and Laurent Nguyen[1]*

[1]GIGA-Neurosciences, Interdisciplinary Cluster for Applied Genoproteomics (GIGA-R), University of Liège, C.H.U. Sart Tilman, Liège, Belgium. [2]Institut Pasteur, Biology of Infection Unit, Paris, France. [3]Inserm U1117, Paris, France. [4]BIOMED - Hasselt University, Hasselt, Belgium. [5]Département d'Histologie-Embryologie-Cytogénétique, Hôpital Necker-Enfant Malades, Paris, France. [6]Inserm U 1163 Institut Imagine, Paris, France. [7]Université Libre de Bruxelles (ULB), Institute for Interdisciplinary Research in Human Biology (IRIBHM), and ULB Institute of Neuroscience (UNI), Brussels, Belgium. [8]Institut Pasteur, Structural Virology Unit, Paris, France. [9]WELBIO, Université Libre de Bruxelles, Brussels, Belgium. [10]Paris Descartes University, Sorbonne Paris Cité, Division of Infectious Diseases and Tropical Medicine, Necker-Enfants Malades University Hospital, Institut Imagine, Paris, France. Ivan Gladwyn-Ng, Lluis Cordon Barris, Christian Alfano, Catherine Creppe and Thérèse Couderc contributed equally to this work. *e-mail: marc.lecuit@pasteur.fr; lnguyen@ulg.ac.be

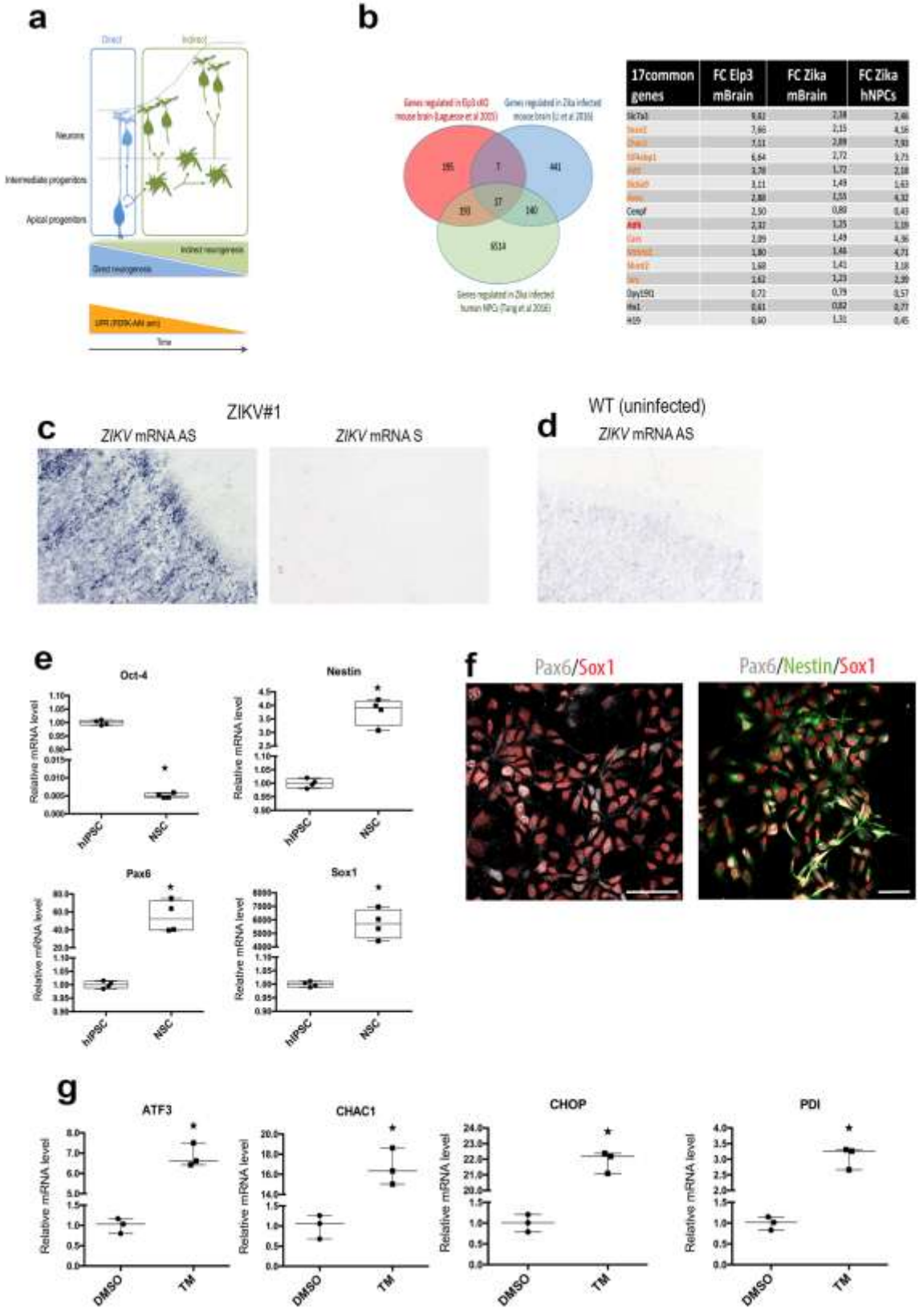

Supplementary Figure 1

ZIKV infection triggers ER stress in human cortices and hNSCs

a, Model of cortical neurogenesis related to UPR.

b, Venn diagram, and top regulated genes common to three models studying microcephaly upon ZIKV infection or activation of ER stress.

c-**d**, Expression pattern of ZIKV mRNAs in the developing cerebral cortex of an ZIKV-infected fetus (ZIKV#1, 25 GW) detected by antisense (AS) probes but not sense probes (S) (**c**). Uninfected brain (WT, 21GW) does not show ZIKV mRNA signal (**d**) (n = 3 independent experiments).

e-**f**, Human neural stem cells (hNSCs) analyzed by qRT-PCR (n = 4 biologically independent samples) to detect *OCT4* (*P = 0.0286, U = 0), *NESTIN* (*P = 0.0286, U = 0), *PAX6* (*P = 0.0286, U = 0), and *SOX1* (*P = 0.0286, U = 0) (**e**). Immunolabelings of PAX6 (grey), SOX1 (red) and NESTIN (green) (n = 3 biologically independent samples) (**f**).

g, Boxplots showing increased expression of *ATF3* (*P < 0.05, U = 0), *CHAC1* (*P < 0.05, U = 0), *CHOP* (*P < 0.05, U = 0), and *PDI* (*P < 0.05, U = 0) upon tunicamycin treatment (TM) (n = 3 biologically independent samples).

e-g, Data are presented as boxplots of median ± first to third quartiles while whiskers extend to maxima and minima with each symbol representing one biologically independent sample (n = 3 to 4) as indicated on boxplots and analyzed by either two-sided (**e**) or one-sided (**g**) Mann-Whitney test.

Scale bars represent 50µm (**f**). *P<0.05.

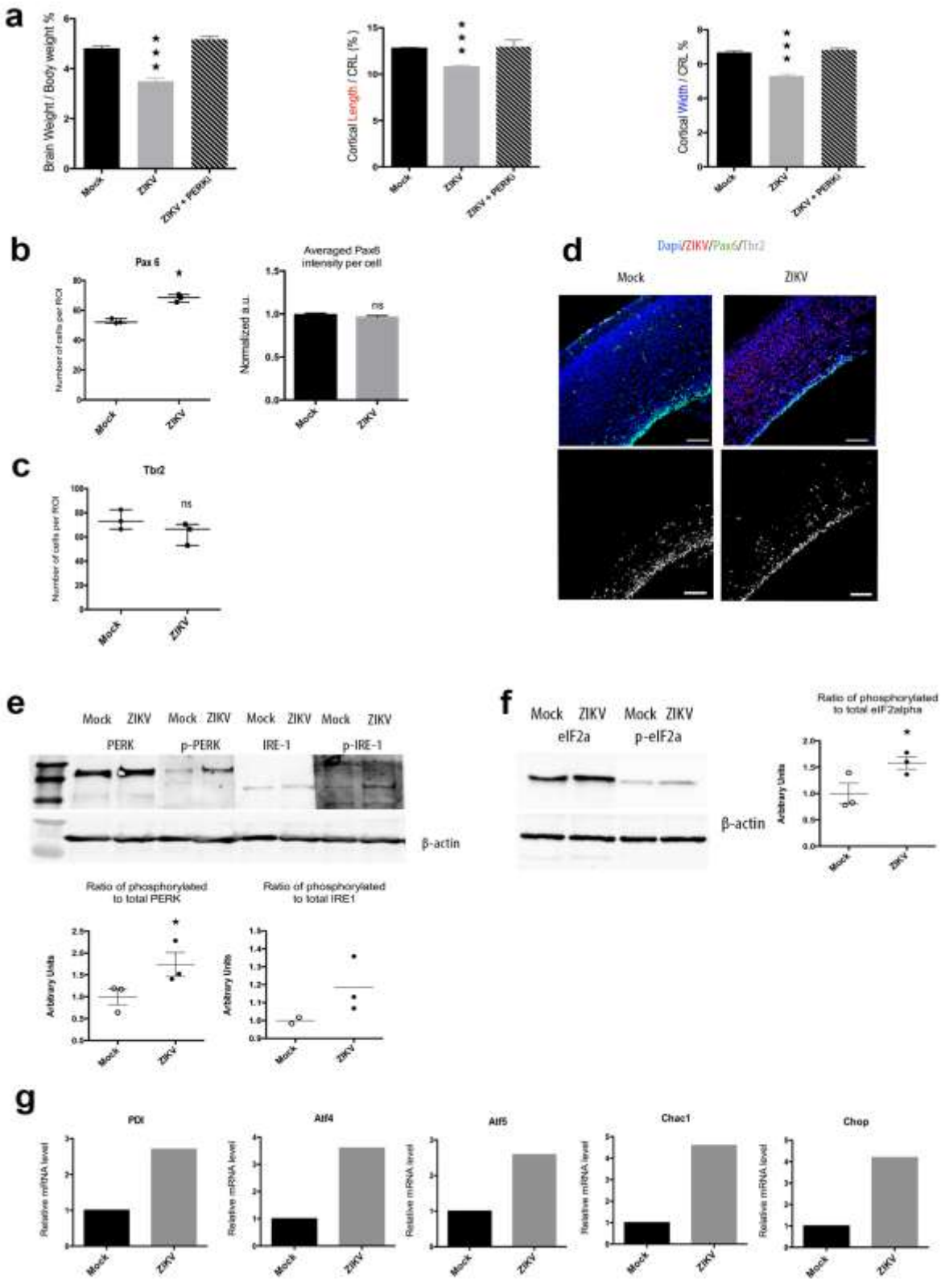

Supplementary Figure 2

Activation of PERK and IRE-1 pathways in ZIKV infected mouse brains from WT or *Ifnr*-knockout mice induce ER stress and microcephaly

a, Intracerebroventricular (ICV) co-injection of ZIKV and PERKi at E12.5 rescues microcephaly of newborn pups. Data are presented as histograms and error bars of mean ± SEM respectively and analyzed by one-way ANOVA followed by Bonferonni *post hoc* comparison test to compare brain weight ($F_{2,43}$=59.06, P<0.0001), normalized cortical length ($F_{2,43}$=65.85, P<0.0001), and cortical width ($F_{2,43}$=74.12, P<0.0001) of pups after Mock, ZIKV or ZIKV + PERKi as indicated on the x-axes (14, 14, 16 brains from separate litters respectively) (**a**).

b-**d**, Histograms and related immunolabelings showing that ICV ZIKV injection into E12.5 brains increases number of Pax6+ (*P < 0.05, U = 0) but not Tbr2+ (P = 0.150, U = 1.5) cells in E18.5 cortices (n = 7 to 9 animals); the averaged Pax6-intensity remains unchanged (P = 0.9172, U = 20) between conditions (n = 96 to 106 cells from 3 independent embryonic brains) (**b-c**). Immunolabelings showing Dapi (blue), ZIKV (red) Pax6 (green), and Tbr2 (grey) (n = 7 to 9 independent embryonic brains) (**d**). Data are presented as boxplots of median ± first to third quartiles while whiskers extend to maxima and minima with each symbol representing independent embryonic brains (n = 3) as indicated and analyzed by two-sided Mann-Whitney test (**b-d**).

e-**f**, Western blot analyses of proteins extracted from E15.5 mouse brains ICV injected with Mock or ZIKV at E12.5. Representative immunoblots showing increased phosphorylation of PERK (*P < 0.05, U = 0) and IRE-1in ZIKV-infected brains and quantification of phosphorylated/unphosphorylated protein ratio after normalization of individual samples (n = 2 to 3 independent embryonic brains) with respect to corresponding conditions (**e**). Immunoblot and corresponding scatter-plots showing increased phosphorylation of eIF2a protein (n = 2 to 3 independent embryonic brains, *P < 0.05, U = 0) (**f**). Data are presented as scatter-plots of means ± SEM with each symbol representing biologically independent samples as indicated on and analyzed by two-sided Mann-Whitney test (**e-f**).

g, Corresponding histograms representing fold change of UPR factor transcripts in E14.5 brains from an Ifnr-/- dam intraperitoneally injected with ZIKV at gestational day 9.5. Microdissected cortices were analyzed by qRT-PCR to detect *PDI*, *Atf4*, *Atf5*, *Chac1*, and *Chop*; one representative experiment for each condition.

Scale bar represents 100 µm (**d**). ***P<0.001, and *P<0.05.

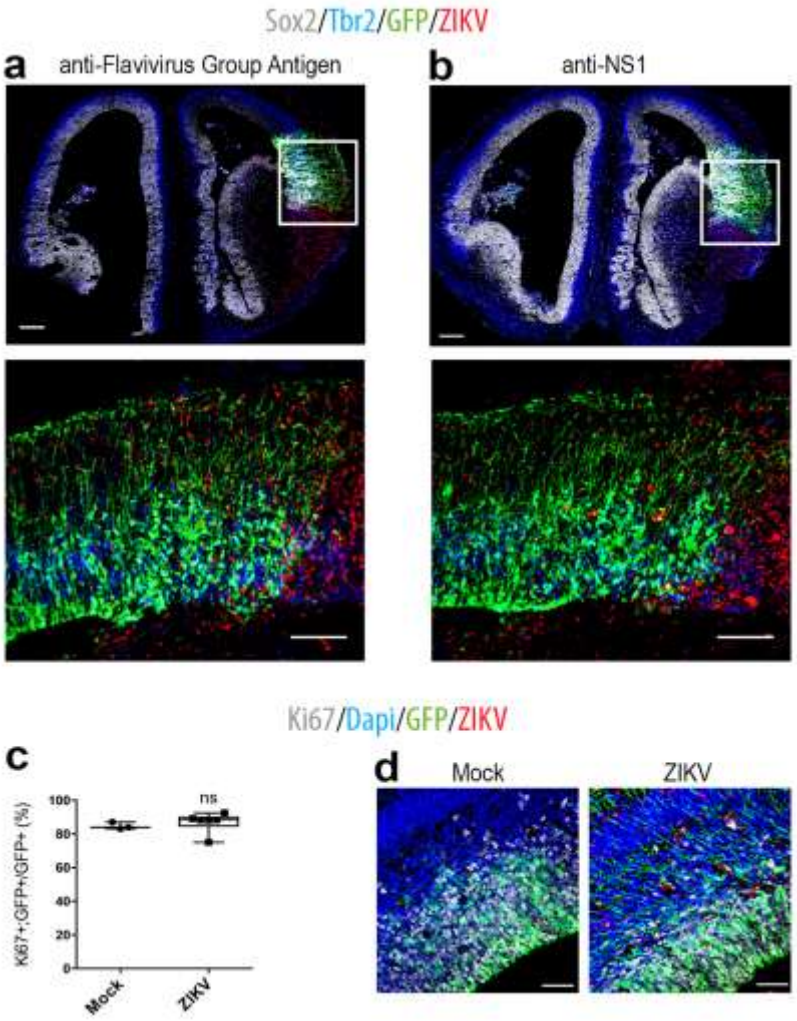

Supplementary Figure 3

Comparison of the expression pattern of ZIKV using two types of antibodies and proliferation assessment

a-b,Immunolabelings of brain slices from E14.5 embryos infected by ZIKV after intracerebroventricular injection at E12.5 and followed by *in utero* electroporation of GFP at E13.5. Immunolabelings show Tbr2 (blue), Sox2 (light grey), GFP (green), and ZIKV (red, using two types of antibodies, as indicated in **a** and **b**) (n = 3 independent experiments from 3 different embryonic brains).

c-d, Assessment of proliferation rate (Ki67+, white) of GFP+ apical progenitors (green) in Mock condition or after ZIKV infection (red). Nuclei are counterstained with Dapi (blue) (n = 3 to 6 independent experiments) (**c**-**d**). Data is presented as boxplot of median ± first to third quartiles while whiskers extend to maxima and minima with each symbol representing independent embryonic brains (n = 3 to 6, $P < 0.116$, $U = 3$), as indicated on boxplots and analyzed by two-sided Mann-Whitney test (**c**).

Scale bar represent 200µm (**a**, **b**), 100µm (boxed regions in **a** and **b**), or 50µm (**d**). ns means not significant.

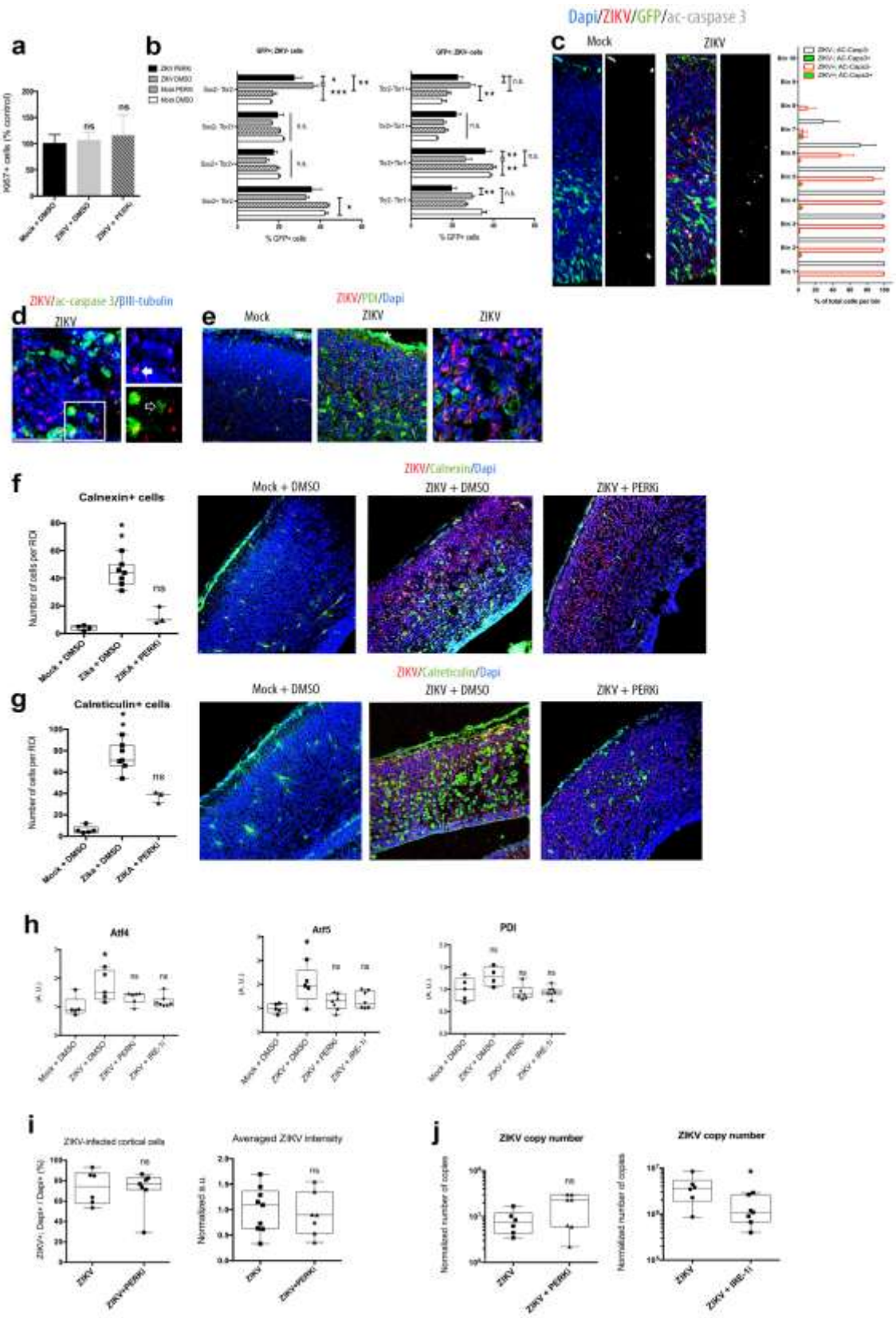

Supplementary Figure 4

ZIKV does not impair cell survival after 2 d but leads to PERKi-sensitive ER stress

a, Data presented as histograms and error bars of mean ± SEM respectively and analyzed by one-way ANOVA followed by Bonferonni *post hoc* comparison test, representing cycling progenitors that express Ki67 and expressed as percentage of control, experimental conditions as mentioned on the graph (n = 11 independent embryonic E14.5 brains per condition infected at E12.5) (**a**).

b-c, ZIKV induces non-cell autonomous changes of the neurogenic balance in E14.5 brains after infection at E12.5 (n = 4 to 5 independent embryonic brains, Sox+Tbr2+, $F_{9,56}$=8.717, *P*<0.0001; Tbr2+Tbr1+, $F_{9,56}$=8.883, *P*<0.0001) (**b**). Immunolabelings of brain slices from E14.5 embryos showing Dapi (blue), ac-caspase 3 (gray), GFP (green), and ZIKV (red) and related data showing the percentage of cells per bin that express either ZIKV, ac-caspase 3, or co-express the combination of markers as indicated (n = 4 to 5 independent embryonic brains) (**c**). Data presented as histograms and error bars of mean ± SEM respectively and analyzed by two-way ANOVA followed by Bonferonni *post hoc* comparison test.

d-e, Immunolabelings on E14.5 cortical slices from 8 ZIKV-infected E14.5 brain showing ZIKV (red), βIII-tubulin (blue) and ac-caspase 3 (green) (n = 3 independent embryonic brains) (**d**, areas show ZIKV-infected (white arrow) and uninfected (open arrow dying neurons). Immunolabelings on E18.5 cortical slices from Mock or ZIKV-infected E18.5 brain showing ZIKV (red), PDI (green), and Dapi (blue) (n = 3 independent embryonic brains) (**e**).

f-h, treatment with PERKi reduces markers for ER stress in E18.5 brains after ICV injection at E12.5. Immunolabelings of cortical sections from Mock, ZIKV, or ZIKV+PERKi injected brains (5, 7 and 3 brains from separate litters per condition, respectively) to detect Dapi (blue), ZIKV (red), Calnexin (green) (**f,** $F_{2,14}$=11.00, *P*<0.0001), and Dapi (blue), ZIKV (red), Calreticulin (green) (**g,** $F_{2,14}$=12.02, *P*<0.0001) (n = 3 to 7 independent experiments). qRT-PCR performed on total RNA extract from E18.5 micro-dissected cortices after ICV injection of ZIKV at E12.5 to detect the following ER stress or UPR actors: *Atf4* ($F_{3,23}$=8.319, *P*=0.0399), *Atf5* ($F_{3,24}$=8.008, *P*=0.0458), and *PDI* ($F_{3,22}$=6.888, *P*=0.0756) (**h**). Data are presented as boxplots of median ± first to third quartiles while whiskers extend to maxima and minima with each symbol representing independent embryonic brains (n = 3 to 7) as indicated, and analyzed by Kruskal-Wallis followed by Dunn's *post hoc* comparison test (**f-h**).

i, Data are presented as boxplots of median ± first to third quartiles while whiskers extend to maxima and minima with each symbol representing independent embryonic brains (n = 6 to 9) as indicated, indicating the percentage of cortical cells infected by ZIKV (*P* = 0.9172, *U* = 20) and the average ZIKV-intensity (*P* = 0.6870, *t* = 0.4115, *df* = 14), and analyzed by either two-sided Mann-Whitney or unpaired two-tailed Student's *t* test respectively, in infected cells from ZIKV and ZIKV+PERKi injected brains (**i**).

j, Data is presented as boxplots of median ± first to third quartiles while whiskers extend to maxima and minima with each symbol representing independent embryonic brains (n = 6 to 7 brains from separate litters) as indicated, and analyzed by unpaired two-tailed Student's *t* test, indicating the number of viral copies after *in utero* co-injection of either ZIKV, ZIKV+PERKi (*P* = 0.1141, *t* = 1.716, *df* = 11) or ZIKV+IRE-1i (*****P* = 0.0364, *t* = 2.382, *df* = 14) in brain extracts (**j**).

*******P*`<0.001, ******P*<0.01,*****P*<0.05; ns means not significant. Scale bars are 50µm (**d**, **e**).

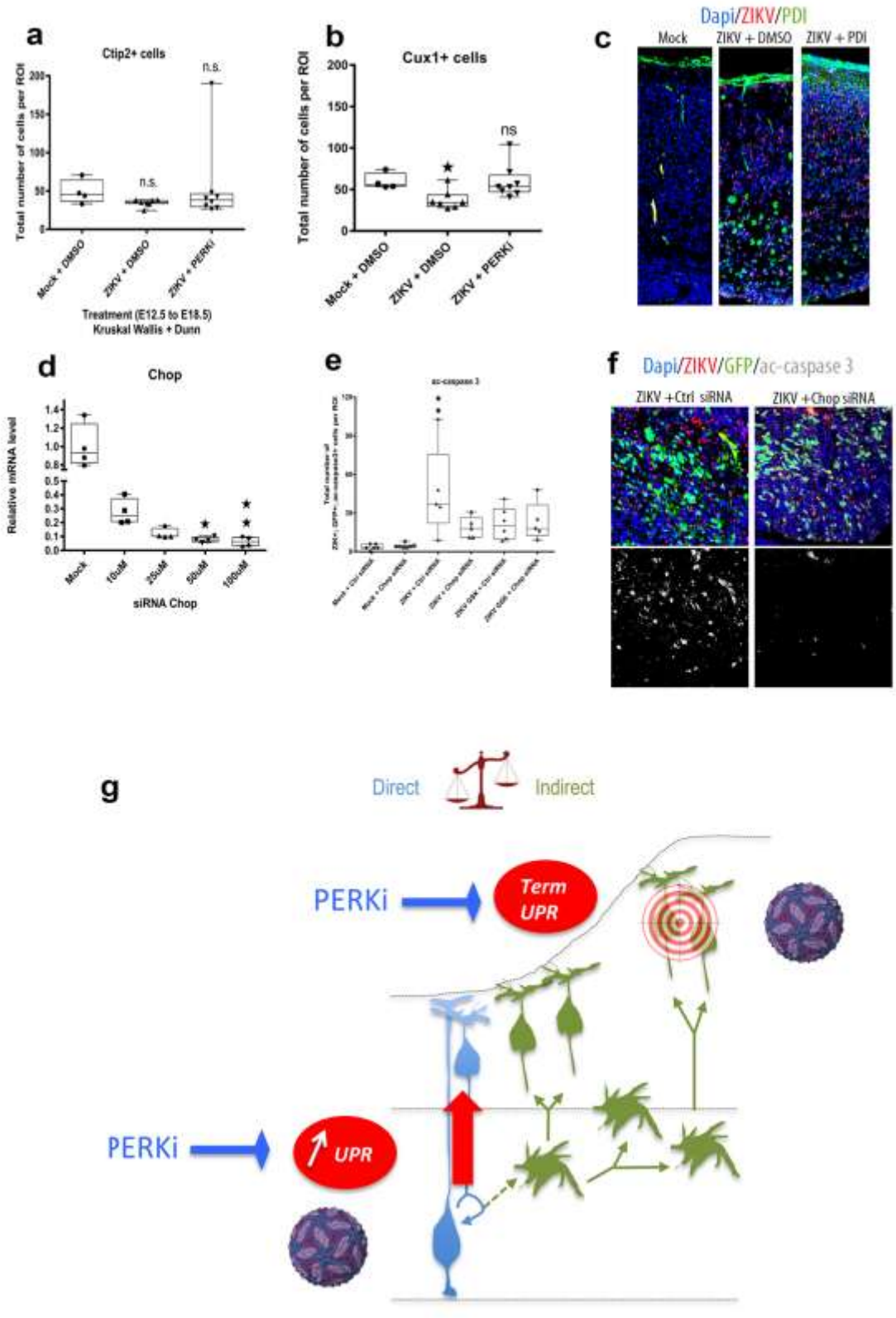

Supplementary Figure 5

ZIKV triggers apoptosis via induction of terminal UPR and expression of *Chop*

a-**b**, Data showing number of Ctip2+ ($F_{2,19}$=2.750, *P*=0.2614) (**a**) and Cux1+ ($F_{2,19}$=7.665, *P*=0.0140) (**b**) cortical neurons in E18.5 brains after treatment with inhibitors as indicated, and presented as boxplots of median ± first to third quartiles while whiskers extend to maxima and minima with each symbol representing one independent sample (n = 4 to 8) as indicated on boxplots, and analyzed by Kruskal-Wallis followed by Dunn *post-hoc* tests.

c, Representative images of immunolabeled coronal sections from brains of E18.5 embryos infected by ZIKV at E12.5 treated by co-injection of DMSO or PERKi with detection of Dapi (blue), ZIKV (red), PDI (green) (n = 5 independent embryonic brains per condition).

d-**e**, Suppression of Chop, a terminal downstream target of PERK pathway, improves survival of ZIKV-infected cortical cells. Boxplot demonstrating *Chop* siRNA suppresses *Chop* expression in transiently transfected Neuro2A cells followed by qRT-PCR (n = 4 independent experiment per condition, $F_{4,20}$=16.53, *P*=0.0024) (**d**). Boxplot demonstrating the comparison of the percentages of ac-caspase 3+ cells in E16.5 mouse brains, after ICV injection of either ZIKV or ZIKV+PERKi at E12.5 followed by *in utero* co-electroporation of either Chop or control siRNA with pCAGGS-GFP (n = 5 embryonic brains per condition, $F_{5,34}$=24.69, *P*=0.0002) (**e**). Data presented as boxplots of median ± first to third quartiles while whiskers extend to maxima and minima with each symbol representing one biologically independent sample as indicated on boxplots, and analyzed by Kruskal-Wallis followed by Dunn *post hoc* comparison test.

f, Representative images of immunolabeled coronal sections from brains of E18.5 embryos infected by ZIKV at E12.5. ZIKV+control siRNA or ZIKV+Chop siRNA E18.5 brains with detection of Dapi (blue), ZIKV (red), GFP (green) and ac-caspase 3.

g, Schematic representation of the mechanisms triggered by ZIKV in the developing cortex. By targeting the APs, ZIKV generates ER stress that raises UPR, leading to an overall reduction of the neuronal output as a result of increased direct neurogenesis (red Arrow). Infected projection neurons suffer from chronic ER stress that activates the UPR target Chop to promote apoptosis (target). Single in vivo injection of PERKi at the time of infection partially releases both pathophysiological events and prevents microcephlay in mouse embryos.

Scale bar represent 100µm (**c**), or 50µm (**f**). $^{**}P<0.01$, and $^{*}P<0.05$; ns means not significant. ROI = region of interest.

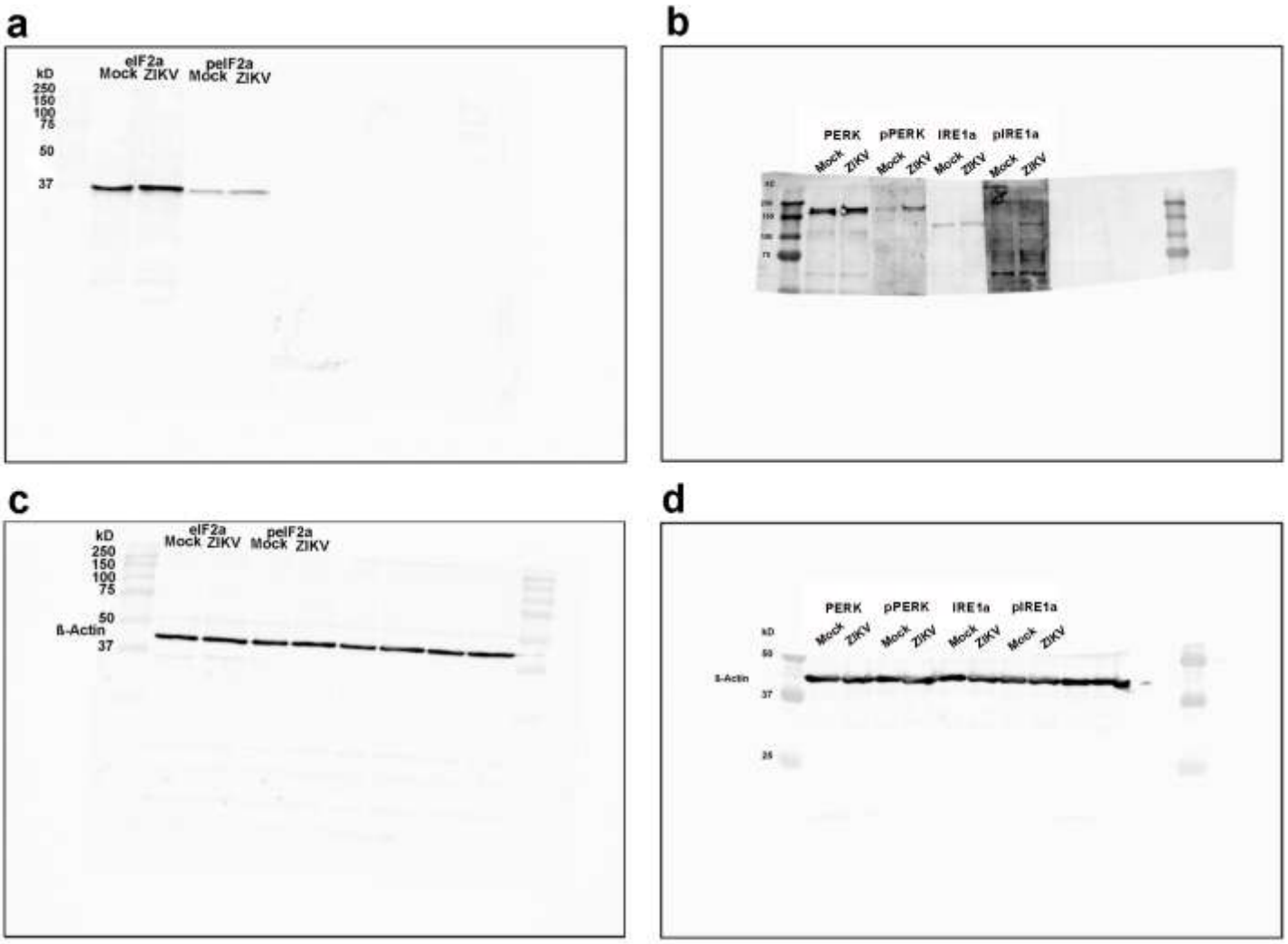

Supplementary Figure 6

Full scans of the western blots presented in Supplementary Fig. 2.

Full scans of the blots immunolabeled for eIF2a and pEIF2a (**a**), PERK, pPERK, IRE1a and pIRE1a (**b**), and ß-Actin (**c** and **d** controls of **a** and **b,** respectively). Each blotting membrane has been cut in several fragments to perform independent immunodetections. These fragments have been manually assembled to reconstitute the original membrane before the scanning.